

Mechanism-based Inhibition Reveals Transitions between Two Conformational States in the Action of Lysine 5,6-Aminomutase: A Combination of Electron Paramagnetic Resonance Spectroscopy, Electron Nuclear Double Resonance Spectroscopy, and Density Functional Theory Study

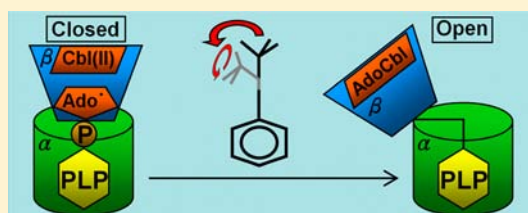
Yung-Han Chen,[†] Amarendra N. Maity,[†] Perry A. Frey,[‡] and Shyue-Chu Ke*[†]

[†]Physics Department, National Dong Hwa University, Hualien, Taiwan 97401

[‡]Department of Biochemistry, University of Wisconsin-Madison, Madison, Wisconsin 53726, United States

S Supporting Information

ABSTRACT: An “open”-state crystal structure of lysine 5,6-aminomutase suggests that transition to a hypothetical “closed”-state is required to bring the cofactors adenosylcobalamin (AdoCbl) and pyridoxal-5'-phosphate (PLP) and the substrate into proximity for the radical-mediated 1,2-amino group migration. This process is achieved by transaldimination of the PLP–Lys144 β internal aldimine with the PLP–substrate external aldimine. A closed-state crystal structure is not available. UV–vis and electron paramagnetic resonance studies show that homologues of substrate D-lysine, 2,5-DAPn, 2,4-DAB, and 2,3-DAPr bind to PLP as an external aldimine and elicit the AdoCbl Co–C bond homolysis and the accumulations of cob(II)alamin and analogue-based radicals, demonstrating the existence of a closed state. ²H- and ³¹P-electron nuclear double resonance studies, supported by computations, show that the position for hydrogen atom abstraction from 2,5-DAPn and 2,4-DAB by the 5'-deoxyadenosyl radical occurs at the carbon adjacent to the imine, resulting in overstabilized radicals by spin delocalization through the imine into the pyridine ring of PLP. These radicals block the active site, inhibit the enzyme, and poise the enzyme into two distinct conformations: for even-numbered analogues, the cob(II)alamin remains proximal to and spin-coupled with the analogue-based radical in the closed state while odd-numbered analogues could trigger the transition to the open state of the enzyme. We provide here direct spectroscopic evidence that strongly support the existence of a closed state and its analogue-dependent transition to the open state, which is one step that was proposed to complete the catalytic turnover of the substrate lysine.



INTRODUCTION

In nature, aminomutases play important roles in anaerobic catabolism of amino acids. These enzymes catalyze the chemically difficult interchange of an amino group and a hydrogen atom on adjacent carbon atoms. Discovered by Stadtman et al.,¹ lysine 5,6-aminomutase (5,6-LAM) plays such a role in lysine metabolism in *Clostridium sticklandii* by catalyzing the interconversion of D-lysine and 2,5-diaminohexanoic acid (2,5-DAH) and of L- β -lysine and 3,5-diaminohexanoic acid (3,5-DAH), which are eventually degraded into ammonia, acetic acid, and butyric acid. 5,6-LAM also catalyzes, albeit less efficiently, the interconversion of L-lysine and 2,5-DAH. 5,6-LAM is composed of two distinct subunits designated α and β and uses adenosylcobalamin (AdoCbl) and pyridoxal-5'-phosphate (PLP) as cofactors. Chang and Frey² cloned the genes encoding the α and β subunits from *C. sticklandii* and coexpressed them in *Escherichia coli*. Their work makes structural and mechanistic characterization of 5,6-LAM possible, which certainly will add further valuable contribution to the knowledge of AdoCbl-dependent enzymology.³

A substrate-free crystal structure⁴ showed that 5,6-LAM from *C. sticklandii* is an $\alpha_2\beta_2$ tetramer. The PLP is bound by a α -triosephosphate isomerase (α -TIM) barrel likely the active site of 5,6-LAM, and AdoCbl is bound by a β -Rossmann domain (Figure 1A). The PLP also binds to Lys144 β of the β -Rossmann domain as an internal aldimine that tethers the two subunits together. The β -Rossmann domain is tilted toward the edge of the α -TIM barrel, positioning AdoCbl \sim 25 Å away from PLP.⁴ This “edge-on” conformation represents an “open” state of the enzyme allowing substrate to enter presumably through the cleft that leads to the top of the TIM barrel and the PLP. It was proposed that transaldimination by a substrate would release the linkage of PLP to the β subunit and that would allow the β -Rossmann domain to swing directly atop the α -TIM barrel closing the pore. The crystal structure of such a “top-on” conformation representing a “closed” state is not yet available but is believed to be analogous to that of substrate-bound methylmalonyl coenzyme A mutase⁵ (Figure 1B). In the

Received: October 1, 2012

Published: December 12, 2012

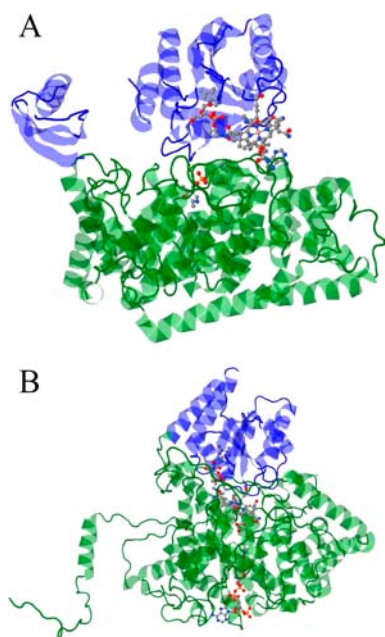


Figure 1. (A) Edge-on vs (B) top-on enzyme conformations.⁴ (A) Structure of the substrate-free form of 5,6-LAM (Protein Data Bank (PDB) code 1XRS) showing edge-on conformation with the β -Rossmann domain and the dimerization domain in blue and the α -TIM barrel and the accessory clamp in green. Cofactors are shown as sticks and spheres. (Figure S1, Supporting Information). (B) Structure of substrate-bound MCM (PDB code 1REQ) showing top-on conformation. Substrate and cofactor are shown as sticks and spheres.

hypothetical closed state, the AdoCbl would be brought into proximity to the substrate-PLP complex, locking all reaction components together for the succeeding radical-mediated 1,2-amino group migration.

The proposed mechanism⁶ for the action of 5,6-LAM is depicted in Figure 2. Step 1 is substrate binding as the

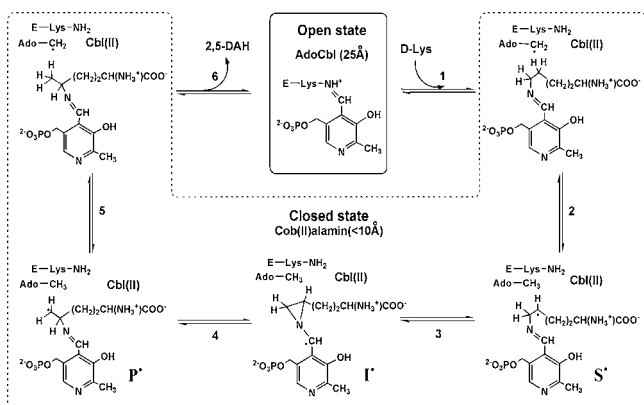


Figure 2. Hypothetical mechanism for the action of 5,6-LAM.

substrate-PLP external aldimine is believed to trigger the β -Rossmann domain top-on movement leading to the closed state. This motion is also assumed to cause the homolytic cleavage of the Co-C bond of AdoCbl and generation of the 5'-deoxyadenosyl radical (S' -Ado \cdot) and cob(II)alamin. In step 2, C5(H) abstraction from the substrate-PLP aldimine by the S' -Ado \cdot generates a substrate-PLP-based radical (S^\bullet) and S' -AdoH. In steps 3 and 4, S^\bullet isomerizes to a product-PLP based-radical (P^\bullet) via a hypothetical cyclic azacyclopropylcarbinyl

radical (I^\bullet). In step 5, P^\bullet accepts a hydrogen atom from S' -AdoH to generate the product-PLP aldimine and S' -Ado \cdot . In step 6, transition to the open state is accompanied by reformation of the PLP-Lys144 β internal aldimine and intact AdoCbl. The open state allows the release of a product and binding of a new substrate, and that completes the catalytic cycle.

The radical mechanism proposed for 5,6-LAM is analogous to that for lysine 2,3-aminomutase (LAM),^{3b,e,7} which catalyzes PLP, S-adenosylmethionine, and an iron-sulfur cluster assisted isomerization of α -lysine into β -lysine. However, unlike LAM and most AdoCbl-dependent enzymes,⁸ no radical species proposed in Figure 2 could accumulate to spectroscopically detectable levels, due to the inherent lack of sufficient stabilities. The only spectroscopic evidence^{9a,b} that supports the radical mechanism was given by electron paramagnetic resonance (EPR) observation of a transient C5-based radical (S^\bullet) and a cob(II)alamin in a spin-coupled manner, using 4-thia-lysine (4-S-2,6-DAH) as an alternative substrate. The sulfur in place of C4 stabilizes the unpaired electron at C5 by spin delocalization. The EPR estimated separation distance of ~ 7 Å between C5 and Co^{II} in cob(II)alamin supports the presence of a closed state. Spin delocalization from C5 to S4 also increases the potential barriers to form the azacyclopropylcarbinyl radical toward a product or to return to the substrate at a significant rate, and that leads to tautomerization of the transient radical into a persistent radical,⁹ in which a C6(H) of the transient radical is transferred to the carboxaldehyde carbon (C4') of PLP. The persistent radical remains spin-coupled with the low spin Co^{II} with a separation distance of ~ 10 Å and blocks the active site in the closed state.

To date, spectroscopic evidence on the proposed transition of a closed state to an open state is not yet available, which is of fundamental importance toward understanding how the enzyme triggers the reformation of the PLP-Lys144 β internal aldimine and product release. Recently, an elegant computational study was performed on another AdoCbl- and PLP-dependent enzyme, ornithine 4,5-aminomutase,¹⁰ to elucidate the synergy between a similar open to closed conformational movement and homolytic cleavage of Co-C bond of AdoCbl, but no attention was given on the transition of a closed state to an open state.

In this study, we present EPR results of a series of homologues of D-lysine (Figure 3) in reaction with 5,6-LAM that supports the presence of a closed state and demonstrates an unprecedented relation between the even- and odd-numbered analogues and the β -Rossmann closed to open domain movement. Electron nuclear double resonance

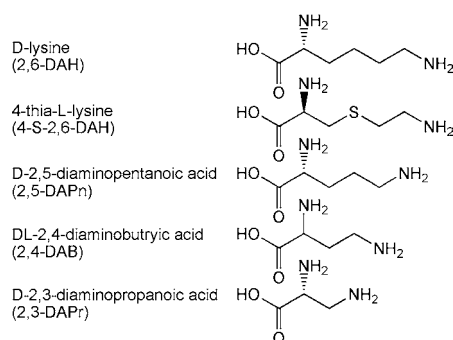


Figure 3. Compound structures and abbreviations.

(ENDOR) spectroscopy and density functional theory (DFT)-based computation were employed to assist in radical structure assignments and in understanding the inactivation mechanism.

MATERIALS AND METHODS

Materials. D-2,6-Diaminohexanoic acid, 4-thia-L-lysine, D-2,5-diaminopentanoic, DL-2,4-diaminobutyric, D-2,3-diaminopropanoic acids, and other chemicals were obtained commercially. $[4'-^2\text{H}]$ PLP was synthesized following the literature procedure for $[4'-^3\text{H}]$ PLP.¹¹

WT 5,6-LAM. The recombinant 5,6-LAM from *C. sticklandii* was produced by expression in *E. coli* and purified following previous procedures.²

UV–Vis Measurements. The holoenzyme mixture and bulk solution containing substrate/analogue were purged and saturated with argon, followed by aerobic measurement of optical responses by a Shimadzu UV-2550 UV–vis spectrophotometer.

EPR/ENDOR Measurements. EPR data were collected using a Bruker EMX spectrometer equipped with a Bruker TE₁₀₂ cavity. The microwave frequency was measured with a Hewlett–Packard 5246L electronic counter. ENDOR spectra were recorded with a Bruker DICE ENDOR assembly equipped with a Bruker TM₁₁₀ cavity. The temperature was controlled by an Advanced Research System Helitran continuous flow cryostat (3.2–200 K). EasySpin¹² was employed to simulate the spectra.

Computations. Geometry optimizations were performed in the gas phase at the B3-LYP level with 6-31G(d,p) basis. Improved relative energies at 0 K were evaluated at the RMP2/G3MP2large level. A factor of 0.9806 was used to scale the zero-point energies. The hyperfine coupling constants were calculated with B3-LYP/6-311G-(2d,p).¹³ These levels of theory have provided many insights for adenosylcobalamin and PLP-assisted reactions.^{13,14}

The methyl group and the phosphate handle of PLP were replaced with hydrogen atoms. N1 of the pyridine ring of PLP is not protonated as suggested by the crystal structure⁴ of 5,6-LAM. The substrate and analogue structures were not truncated. Previous study showed that only a small amount of net charge can be found on the carboxylate group that is interacting with a positively charged protein residue.¹⁵ Therefore, we have chosen neutral α -carboxylic acid and amine groups as our gas-phase model to imitate their possible interactions with the protein. Fully optimized structures were characterized by the absence of imaginary vibrational frequencies. The Gaussian 03 suite of programs¹⁶ was used for all calculations.

RESULTS

UV–Vis Spectroscopy. Figure 4 shows that addition of substrate or analogue causes decreases in the absorbance at 423 nm, a characteristic band for PLP–Lys144 β internal aldimine, and slight redshifts to 432 nm, indicating the capability of PLP to form external aldimine with the analogues. Addition of substrate or analogue also decreases the absorbance at 380 and 523 nm, characteristic bands for AdoCbl, reflecting their abilities to elicit Co–C bond homolysis rather than binding passively. The increases of the absorbance between 310 and 350 nm suggests that none of the analogue–PLP undergo internal transaldimination with the α -amino group. No spectra component at \sim 500 nm due to accumulated quinonoid intermediate is evident.

EPR Spectroscopy. Figure 5a shows the EPR spectrum generated in the reaction of 5,6-LAM with 4-S-2,6-DAH at 3 min. The spectrum along with its isotope-edited effects has been characterized well⁹ and is included here for comparison with other substrate–analogue-induced EPR spectra. In brief, the spectrum is due to the presence of a persistent radical spin-coupled with the low-spin Co^{II} of cob(II)alamin at a separation distance of \sim 10 Å; thus, the spectrum is indicative of a closed state of the enzyme.

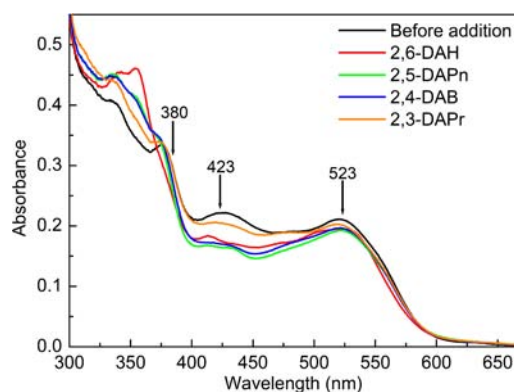


Figure 4. UV–vis spectra changes in the reaction of 5,6-LAM with substrate and analogues. The holoenzyme solution contained 25 μM 5,6-LAM, 25 μM PLP, and 25 μM AdoCbl in 100 mM NH_4EPPS buffer at pH 8.5 in a total volume of 1 mL. Holoenzyme (black line). Spectra changes were recorded at 25 °C at 3 min after addition of 20 mM 2,6-DAH (red line), 2,5-DAPn (green line), 2,4-DAB (blue line), and 2,3-DAPr (orange line).

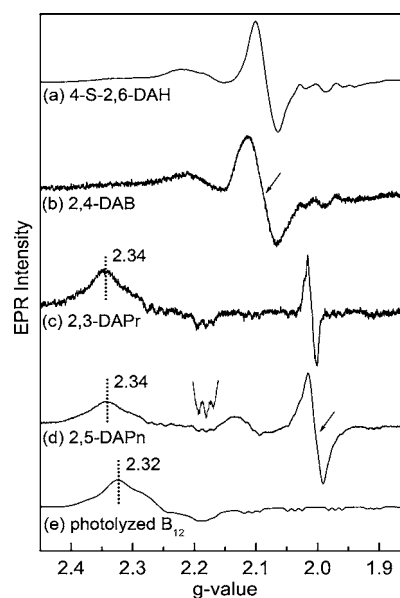


Figure 5. 77 K EPR spectra for radicals generated in the reaction of 5,6-LAM with 4-S-2,6-DAH, 2,4-DAB, 2,3-DAPr, and 2,5-DAPn (from top to bottom). 5,6-LAM at 0.3 mM was incubated with 100 mM NH_4EPPS buffer (pH 8.5), 5 mM dithiothreitol, 0.3 mM AdoCbl, and 0.3 mM PLP at 37 °C. The reaction was initiated by addition of 30 mM analogues and allowed to proceed for 3 min aerobically. Spectrum (e) is photolyzed AdoCbl in solution. Arrows mark the positions for ENDOR measurements. Instrument settings: microwave frequency, 9.6 GHz; microwave power, 20 mW; modulation amplitude, 4 G at 100 kHz.

Unlike the existence of a transient radical trapped in the reaction of 5,6-LAM with 4-S-2,6-DAH at <10 s (data not shown),^{9a,b} the EPR lineshapes derived from the reaction of 5,6-LAM with 2,3-DAPr, 2,4-DAB, or 2,5-DAPn are persistent within 20 min indicating the stabilities of these radicals. Figure 5b shows the EPR spectrum of a persistent radical generated in the reaction of 5,6-LAM with 2,4-DAB. The spectrum pattern resembles that generated with 4-S-2,6-DAH (Figure 5a) and thus is attributed to the presence of a stable 2,4-DAB-based radical spin-coupled with the low-spin Co^{II} in cob(II)alamin at a separation distance of \sim 10 Å as well. This demonstrates that,

in the reaction with 2,4-DAB, the enzyme remains in a closed state as with that in reaction with 4-S-2,6-DAH. The similarity of the two spectra also suggests that sulfur does not induce obvious strain into the active site.

The EPR spectrum generated with 2,3-DAPr (Figure 5c) is entirely different. The spectrum shows no trace of spin-coupled signal and is interpreted as a sum of two separate EPR identities: 2,3-DAPr-based persistent radical at $g \sim 2$ and Co^{II} in cob(II)alamin at $g_{\perp} \sim 2.34$ and an octet pattern superimposed by a ^{14}N triplet hyperfine splitting centered at $g_{\parallel} \sim 2$. The g value of the g_{\perp} transition is consistent with previous data for AdoCbl in 5,6-LAM treated with methylhydrazine² in the precatalytic open state and also appears with a value larger than that of photolyzed AdoCbl in solution (Figure 5e, $g_{\perp} \sim 2.32$), demonstrating that cob(II)alamin remains bound to the enzyme. The fact that the 2,3-DAPr-based radical is not spin-coupled with the Co^{II} in cob(II)alamin thus signifies an open state of the enzyme. However, whether or not the structure of such an open state is identical to that of the precatalytic open state (Figure 1a) cannot be ascertained.

The EPR spectrum of the radical species with 2,5-DAPn is shown in Figure 5d. The spectrum exhibits the presence of both the uncoupled Co^{II} and the 2,5-DAPn-based radical (major) and their spin-coupled ensemble at $g \sim 2.11$ (minor). That is, addition of 2,5-DAPn to the holoenzyme mixture have resulted in two distinct enzyme conformations: a majority portion in the open state and a smaller portion in the closed state, with cob(II)alamin in proximal to and spin-coupled with the 2,5-DAPn-PLP derived radical. Explanation to the coexistence of both states will be discussed later.

The EPR data presented here clearly demonstrate that odd-numbered substrate analogues (2,5-DAPn and 2,3-DAPr) are capable of triggering the transition from the closed state to an open state, while with even-numbered analogues (4-S-2,6-DAH and 2,4-DAB) the enzyme remains in the closed state.

ENDOR Spectroscopy. ENDOR spectroscopy was employed to aid in radical structure assignments and to investigate whether transition to the open state in the case of 2,5-DAPn requires decomposition of the analogue-PLP aldimine. The ENDOR spectrum with 2,4-DAB (Figure 6.1) is collected at 3318 G corresponding to the maximum absorption of the EPR signal (Figure 5b). The spectrum resembles the previously reported spectrum generated with 4-S-2,6-DAH.^{9c} The two pairs of transitions at (4.6, 6.2) and (5.53, 5.9) MHz are attributed to ^2H and ^{31}P of $[4\text{'-}^2\text{H}]\text{PLP}$, respectively.

The ENDOR spectra (Figure 6.2) with 2,5-DAPn are collected at 3405 G because in this case the organic radical is spin-uncoupled from cob(II)alamin and thus its EPR absorption appears at higher magnetic field than that with 2,4-DAB. As a result, free Larmor precession of ^{31}P is also shifted to a higher frequency at 5.87 MHz. The pair of signals at 5.58 and 6.16 MHz, mirroring about 5.87 MHz, is assigned to the ENDOR transition of ^{31}P of $[4\text{'-}^2\text{H}]\text{PLP}$. Assignment of the pair of lines at (4.8, 6.54) MHz to ^2H -ENDOR transitions is reinforced by comparison of the sample containing $[4\text{'-}^2\text{H}]\text{PLP}$ (Figure 6.2b) with that of unlabeled sample (Figure 6.2a).

The simulated ENDOR parameters are presented in Table 1. The 2,5-DAPn-PLP-based radical displays slightly larger hyperfine coupling with the $\text{C4}'(^2\text{H})$, compared to that with 2,4-DAB-PLP. Relatively, the 2,5-DAPn-PLP-based radical displays slightly smaller hyperfine coupling with the ^{31}P in PLP, as also reflected by the less asymmetric ENDOR line shape. We attribute the slight differences in spin distribution to the

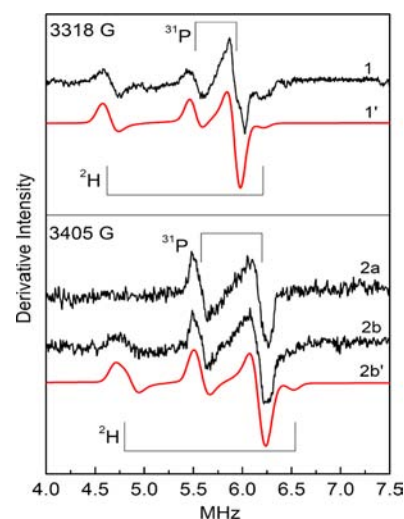


Figure 6. X-band ENDOR spectra (black) along with powder spectra simulation (red) of radical intermediates trapped at 3 min in the reaction of 5,6-LAM with 2,4-DAB (panel 1) and with 2,5-DAPn (panel 2). Coenzyme $[4\text{'-}^2\text{H}]\text{PLP}$ is used in the data collection of spectra 1 and 2b; $[4\text{'-}^1\text{H}]\text{PLP}$ for spectrum 2a. The spectra were taken at the maximum EPR absorption as indicated by arrows in Figure 5. Instrument settings: microwave power, 2 mW; RF power, 200 W; modulation depth, 100 kHz; T , 20 K; magnetic fields are as indicated. For simulation parameters, see Table 1.

consequence of active-site structural variation due to transition to the open state when 2,5-DAPn is used as the substrate analogue.

Overall, ENDOR data are significant in two aspects: (1) the analogue-PLP aldimine remains intact for both analogues apart from the enzymatic state being open or closed; and (2) the spin density in the imine and PLP moiety are approximately equivalent for the two analogues, suggesting that their radical structures are likely alike.

Neither a ^2H - nor a ^{31}P -ENDOR signal can be resolved in the reaction of 5,6-LAM with 2,3-DAPr. Inasmuch as the signal/noise ratio of the ~ 14 MHz feature due to dipolar interactions of the unpaired spin with remote and surrounding solvent protons also appears to be very low (data not shown), which normally is a prominent feature in solid-state ENDOR, we suspect that the lack of detectable ^2H - or ^{31}P -ENDOR signals might be partly due to low concentration of paramagnets in the sample. Due to the lack of ENDOR signals and narrower EPR line width as compared with that of the 2,5-DAPn-PLP-based radical (Figure 5c,d), the possibilities that the unpaired electron to some extent is stabilized by the nearby α -carboxylate group and hence less spin delocalization into the pyridine ring of PLP or simply the radical is not based on 2,3-DAPr-PLP could not be ruled out.

DFT Computation. Figure 7 suggests three possible structures for the 2,5-DAPn-PLP-based radical, and their corresponding theoretical hyperfine coupling constants (HFCCs) of the deuterium at $\text{C4}'$ in PLP, obtained at the B3-LYP/6-311G-(2d,p) level, are given in Table 1. Such a link between theory and experiment has been proven to be useful for identifying radical structures. The possibilities for a quinonoid radical or a radical underwent internal transaldimination are excluded by UV-vis data; these radicals also would not display the observed hyperfine coupling.

Table 1. ^2H and ^{31}P Hyperfine Parameters

analogue	experiment						theory				
	$A(^{31}\text{P})_{\text{ENDOR}}$ (MHz)			$A(^2\text{H})_{\text{ENDOR}}$ (MHz)			radical	atom	$A(^2\text{H})_{\text{DFT}}$ (MHz)		
	A_{xx}	A_{yy}	A_{zz}	A_{xx}	A_{yy}	A_{zz}			A_{xx}	A_{yy}	A_{zz}
D-2,5-DAPn	-0.75	-0.55	14.0	-4.95	-5.30	-8.60	C5	$\text{C4}'(^2\text{H}_\alpha)$	-2.09	-5.40	-7.58
							C4	$\text{C4}'(^2\text{H})$	-0.34	-0.26	0.29
							C4-based tautomer	$\text{C4}'(^2\text{H}_{\beta 1})$	11.46	11.57	12.85
								$\text{C4}'(^2\text{H}_{\beta 2})$	3.10	3.62	4.48
D-2,4-DAB	-0.45	-0.45	19.0	-4.80	-5.00	-8.10	C4	$\text{C4}'(^2\text{H}_\alpha)$	-2.02	-5.37	-7.53
							C3	$\text{C4}'(^2\text{H})$	-0.29	-0.15	0.46
							C3-based tautomer	$\text{C4}'(^2\text{H}_{\beta 1})$	11.00	11.22	12.38
								$\text{C4}'(^2\text{H}_{\beta 2})$	4.35	4.88	5.75

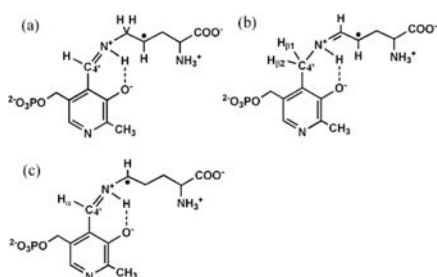


Figure 7. Possible structures for ornithine- N^5 -PLP-aldimine derived radicals. (a) C4 radical, (b) C4-based tautomer radical by transfer of a proton from C5 to C4' of PLP, and (c) C5 radical.

Among the three proposed structures, the experimental $\text{C4}'(^2\text{H})$ values are most close to the theoretical values for a C5 radical (Figure 7c). The coupling is predominantly due to spin polarization of the $\text{C4}'_\alpha\text{H}\alpha$ σ -electron pair bond. The theoretical HFCCs for the C4 radical (Figure 7a) are inconsistent with experiment. We note that the consistency between theory and experiment for the C4-based tautomer (Figure 7b) can be improved by adjusting the β -coupling dihedral angle; after all, the B3LYP gas-phase structure may not always be the actual conformation in biological medium. With 2,4-DAB-PLP, the experimental values are also most close to the theoretical values for a C4 radical. Thus, DFT computations support a radical structure where hydrogen atom abstraction by $5'\text{-Ado}^\bullet$ occurs at the carbon adjacent to the imine for both 2,5-DAPn-PLP and 2,4-DAB-PLP.

Furthermore, EPR data reveal an obvious trend that is in the closed form of 5,6-LAM, odd-numbered analogues could trigger transition to the open state of the enzyme, whereas with even-numbered analogues the enzyme remains in the closed state. To assist in interpreting this trend, we have examined the lowest energy side-chain conformations and their C2 rotameric states of the substrate-PLP, product-PLP, and analogues-PLP complexes. The three consecutive lowest energy structures for each complex are displayed in Figure 8 and will be discussed later. In the absence of structural information on the closed form of the enzyme, we did not take steric restrictions that may be imposed by the active site into consideration, and the side chains are therefore fully extended. The geometry and energy of a true conformation in the active site likely will vary from those given in Figure 8.

DISCUSSION

Radical Structures. The possibility of C4(H) abstraction from 2,5-DAPn-PLP by $5'\text{-Ado}^\bullet$ is ruled out by the following: (1) the C4-based radical (Figure 7a) would proceed through

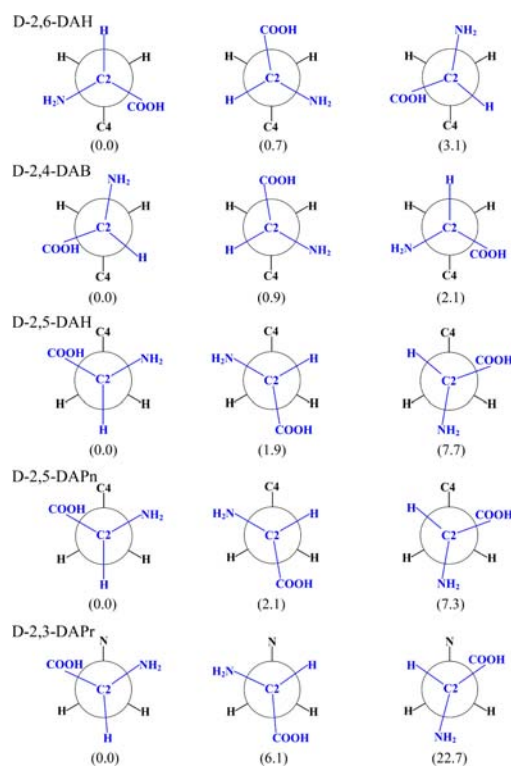


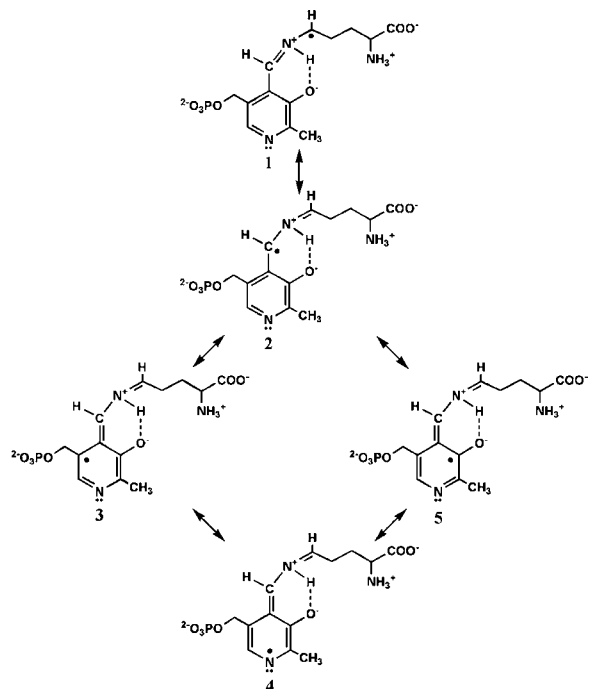
Figure 8. B3-LYP/6-31G(d,p) optimized structures for substrate-, product-, and analogue-PLP complexes displayed by Newman projections through the C2-C3 bond, along with their relative energies (kJ mol^{-1}) at 0 K at the RMP2/G3MP2large level.

the azacyclopropylcarbonyl radical to form product that was not detected and they also would not accumulate to give EPR signals. The reaction energetics along the reaction pathway is likely to be the same as that with substrate 2,6-DAH because their α -carboxylate groups are too remote from the radical center to participate in stabilizing any of the proposed radical intermediates by spin delocalization. (2) The C4 radical would not display significant hyperfine coupling with the ^2H or with the ^{31}P of $[4\text{'-}^2\text{H}]$ PLP (Table 1). (3) Tautomerization of the C4 radical involving transfer of a proton from C5 to C4' of PLP (Figure 7b) could lead to spin delocalization and hence detectable $[4\text{'-}^2\text{H}]$ PLP ENDOR signal, but such a process is not a compulsory process in 5,6-LAM. It is amplified with 4-S-2,6-DAH only because the transient radical is stabilized by the adjacent S4 allowing tautomerization to take place.

Abstraction of C5(H) by $5'\text{-Ado}^\bullet$ leads to a C5 radical (Figure 7c) with properties fully consistent with experimental

and theoretical data reported herein. With the unpaired electron adjacent to the imine and in π conjugation with the pyridine ring of PLP, the resultant is spin delocalization over the entire imine–PLP framework (Scheme 1) and hence a

Scheme 1. Hybrid Forms of the 2,5-DAPn–PLP Radical Derived from Abstraction of C5(H) by S' -Ado $^{\bullet}$



highly stabilized radical. Without the need of any isomerization process, this radical itself would fully accumulate to EPR detectable amounts. With a significant amount of spin densities on C4', large isotropic hyperfine coupling with the deuteron of [4'- ^2H]PLP would be expected, consistent with the ENDOR and DFT data (Table 1). In the present study, the HFCCs of ^{31}P were not calculated (the phosphate handle of PLP is replaced with a hydrogen atom), which would be strongly influenced by the choice of the ionic state of phosphate and the modeling of its multiple interactions with the active site. However, as depicted in Scheme 1 hybrid form 3, the unpaired electron is within three atoms of ^{31}P ; therefore, significant hyperfine coupling with ^{31}P can also be expected (Table 1).

The structure of the radical generated in the reaction of 5,6-LAM with 2,4-DAB is assigned as a C4-based radical in the side chain, on the basis of foregoing considerations. The absence of ENDOR data with 2,3-DAPr prohibits us to make further assignment of its radical structure.

Inactivation Mechanism. The inactivation mechanism that is consistent with all of the observations in the reaction of 5,6-LAM with 2,5-DAPn or 2,4-DAB is as follows: (1) binding of 2,5-DAPn or 2,4-DAB to PLP as 2,5-DAPn- N^5 - or 2,4-DAB- N^4 -PLP-aldimine brings forth Co–C homolysis and the formation of S' -Ado $^{\bullet}$ and cob(II)alamin; (2) S' -Ado $^{\bullet}$ abstracts a hydrogen atom from the carbon adjacent to the imine resulting in a highly stabilized radical that is unable to reabstract a hydrogen atom from S' -deoxyadenosine leaving AdoCbl irreversibly cleaved; and (3) regardless of the enzymatic states, open versus closed, the over stabilized radicals block the active sites and inhibit the enzyme.

Transition between Open and Closed States. We demonstrate that addition of homologues of D-lysine triggers the transition from the open state to the closed state and that results in the formation of PLP–analogue-based radicals and cob(II)alamin. Furthermore, EPR spectra show that odd-numbered analogues could trigger the transition back to the open state whereas with even-numbered analogues the enzyme remains in the closed state. Since the ENDOR data suggests similar spin distribution, thus similar structural conformation, in the imine–PLP moiety of 2,5-DAPn–PLP- and 2,4-DAB–PLP-based radicals, the trend revealed by EPR reflects the importance of the structural conformation at C2 in affecting the open versus closed states of the enzyme. We seek to address this intriguing finding and its relevance to the native process by comparing the analogue side-chain conformation and rotameric states at C2 with that of 2,5-DAH–PLP, which is a catalytic product of 2,6-DAH–PLP and will ultimately generate the open state of the enzyme.

In the absence of closed-state structural information showing details of interactions between the α -carboxylate and the amino groups with the enzyme, the following modeling is hypothetical. Considering that PLP is engaged in multiple contacts with the active-site residues,⁴ our model entails the rigidity of PLP in the active site. The 1,2-shift of the ϵ -amino group of 2,6-DAH–PLP to 2,5-DAH–PLP would not change the interaction of the imine–PLP moiety with the active site but would cause the α -carboxylic acid and the amine groups of 2,5-DAH–PLP to interact with different regions of residues, as depicted by Newman projections (Figure 8, rows 1 and 3). The residues peripheral to the α -carboxylic acid and the amine groups of 2,5-DAPn–PLP and 2,3-DAPr–PLP are the same (Figure 8, rows 4 and 5), and they too are identical to that of 2,5-DAH–PLP but different from that of 2,6-DAH–PLP and 2,4-DAB–PLP (Figure 8, rows 1 and 2). Thus, in the context of lowest energy structure, correlation between the examination of side-chain conformation and C2 rotameric state of the analogues and the trend revealed by EPR supports but does not prove that the electrostatic or steric bulk effect at C2 might play an important role in the β -Rossmann domain movement, closed versus open.

Finally, the EPR spectrum (Figure 5) derived from 2,5-DAPn differs slightly from that of 2,3-DAPr. With 2,5-DAPn, in addition to the two dominant spin-uncoupled EPR signals, there is also a minor spin-coupled signal at $g \sim 2.1$. With 2,3-DAPr, no spin-coupled ensemble is detected. This difference may be in part attributed to the higher degree of rotational freedom at C2 of 2,5-DAPn–PLP due to lower energy differences between their rotameric states, as compared to that of 2,3-DAPr–PLP (Figure 8). As a result, both the lowest and the second lowest energy rotamers of 2,5-DAPn–PLP are populated. The lowest energy rotamer has a conformation identical to that of 2,5-DAH–PLP and has higher populations hence larger EPR signals corresponding to open state of the enzyme, while the second lowest energy rotamer gives rise to the smaller spin-coupled EPR signal corresponding to the closed state of the enzyme.

SUMMARY

Our results are significant in three aspects: (1) we show the abilities of homologues of the substrate D-lysine to bind to PLP, to trigger homolytic cleavage of the Co–C bond of AdoCbl, and to initiate the radical mechanism by hydrogen abstraction from the side chain of the analogues. These observations

strongly support the notion that 5,6-LAM operates via a radical mechanism and the existence of a catalytic closed state of the enzyme. (2) We show that, for 2,5-DAPn and 2,4-DAB, the hydrogen abstraction occurs at the carbon adjacent to the imine resulting in an exceedingly stabilized radical by spin delocalization from the radical center into the PLP ring. These radicals cannot react further leaving the Co–C bond irreversibly cleaved, and that is the basis for the inactivation of 5,6-LAM. (3) We provide the only and direct spectroscopic evidence to demonstrate that a transition from a closed state to the open state is possible with odd-numbered analogues. How such a transition observed with mechanism-based inhibitors is relevant to the native process requires further investigation.

■ ASSOCIATED CONTENT

Supporting Information

Structure of the substrate-free form of 5,6-LAM. Complete citation for the Gaussian 03 suite of programs. This material is available free of charge via the Internet at <http://pubs.acs.org>.

■ AUTHOR INFORMATION

Corresponding Author

ke@mail.ndhu.edu.tw

Notes

The authors declare no competing financial interest.

■ ACKNOWLEDGMENTS

The National Science Council of Taiwan (grant NSC-100-2627-M-259 to S.-C.K.) and the U.S. National Institute of Diabetes and Digestive and Kidney Diseases (grant DK28607 to P.A.F.) supported this research.

■ REFERENCES

- (1) (a) Morley, C. G.; Stadtman, T. C. *Biochemistry* **1970**, *9*, 4890–900. (b) Baker, J. J.; van der Drift, C.; Stadtman, T. C. *Biochemistry* **1973**, *12*, 1054–63. (c) Baker, J. J.; Stadtman, T. C. *B12*; Dolphin, D., Ed.; John Wiley & Sons: New York, 1982; Vol. 2, p 203. (d) Stadtman, T. C. *Adv. Enzymol.* **1973**, *38*, 413.
- (2) Chang, C. H.; Frey, P. A. *J. Biol. Chem.* **2000**, *275*, 106.
- (3) (a) Banerjee, R. *Chemistry and Biochemistry of B12*; Wiley: New York, 1999. (b) Frey, P. A.; Magnusson, O. T. *Chem. Rev.* **2003**, *103*, 2129. (c) Banerjee, R. *Chem. Rev.* **2003**, *103*, 2083. (d) Toraya, T. *Chem. Rev.* **2003**, *103*, 2095. (e) Frey, P. A.; Hegeman, A. D.; Reed, G. H. *Chem. Rev.* **2006**, *106*, 3302. (f) Frey, P. A. *Comprehensive Natural Products II: Chemistry and Biology*; Elsevier: Oxford, U.K., 2010; Vol. 7, pp 501–546.
- (4) Berkovitch, F.; Behshad, E.; Tang, K.-H.; Enns, E. A.; Frey, P. A.; Drennan, C. L. *Proc. Natl. Acad. Sci. U.S.A.* **2004**, *101*, 15870.
- (5) Mancia, F.; Keep, N. H.; Nakagawa, A.; Leadlay, P. F.; McSweeney, S.; Rasmussen, B.; Bosecke, P.; Diat, O.; Evans, P. R. *Structure* **1996**, *4*, 339.
- (6) (a) Tang, K. H.; Chang, C. H.; Frey, P. A. *Biochemistry* **2001**, *40*, 5190. (b) Tang, K. H.; Harms, A.; Frey, P. A. *Biochemistry* **2002**, *41*, 8767. (c) Tang, K. H.; Casarez, A. D.; Wu, W.; Frey, P. A. *Arch. Biochem. Biophys.* **2003**, *418*, 49.
- (7) (a) Frey, P. A.; Reed, G. H. *Biochim. Biophys. Acta, Proteins Proteomics* **2011**, *1814*, 1548. (b) Ballinger, M. D.; Frey, P. A.; Reed, G. H. *Biochemistry* **1992**, *31*, 10782. (c) Miller, J.; Bandarian, V.; Reed, G. H.; Frey, P. A. *Arch. Biochem. Biophys.* **2001**, *387*, 281. (d) Wu, W.; Lieder, K. W.; Reed, G. H.; Frey, P. A. *Biochemistry* **1995**, *34*, 10532. (e) Chang, C. H.; Ballinger, M. D.; Reed, G. H.; Frey, P. A. *Biochemistry* **1996**, *35*, 11081. (f) Wu, W.; Booker, S.; Lieder, K. W.; Bandarian, V.; Reed, G. H.; Frey, P. A. *Biochemistry* **2000**, *39*, 9561.
- (8) (a) Gerfen, G. J.; *Chemistry and Biochemistry of B12*; Banerjee, R., Ed.; Wiley: New York, 1999; p 165. (b) Mansoorabadi, S. O.; Reed, G.

- H. *Paramagnetic Resonance of Metallobiomolecules*; Telser, J., Ed.; American Chemical Society: Washington, DC, 2003; p 82.
- (c) Manzerova, J.; Krymov, V.; Gerfen, G. J. *J. Magn. Reson.* **2011**, *213*, 32. (d) Bothe, H.; Darley, D. J.; Albracht, S. P. J.; Gerfen, G. J.; Golding, B. T.; Buckel, W. *Biochemistry* **1998**, *37*, 4105. (e) Reed, G. H.; Mansoorabadi, S. O. *Curr. Opin. Struct. Biol.* **2003**, *13*, 716. (f) Wang, M.; Warncke, K. *J. Am. Chem. Soc.* **2008**, *130*, 4846.
- (9) (a) Tang, K. H.; Mansoorabadi, S. O.; Reed, G. H.; Frey, P. A. *Biochemistry* **2009**, *48*, 8151. (b) Chen, Y. H.; Maity, A. N.; Pan, Y. C.; Frey, P. A.; Ke, S. C. *J. Am. Chem. Soc.* **2011**, *133*, 17152. (c) Maity, A. N.; Hsieh, C. P.; Huang, M. H.; Chen, Y. H.; Tang, K. H.; Behshad, E.; Frey, P. A.; Ke, S. C. *J. Phys. Chem. B* **2009**, *113*, 12161.
- (10) (a) Pang, J. Y.; Li, X.; Morokuma, K.; Scrutton, N. S.; Sutcliffe, M. J. *J. Am. Chem. Soc.* **2012**, *134*, 2367–2377. (b) Wolthers, K. R.; Levy, C.; Scrutton, N. S.; Leys, D. J. *Biol. Chem.* **2010**, *285*, 13942.
- (11) Fu, M.; Silverman, R. B. *Bioorg. Med. Chem.* **1999**, *7*, 1581.
- (12) Stoll, S.; Schweiger, A. *J. Magn. Reson.* **2006**, *178*, 42.
- (13) Wetmore, S. D.; Smith, D. M.; Radom, L. *J. Am. Chem. Soc.* **2001**, *123*, 8678.
- (14) (a) Sandala, G. M.; Smith, D. M.; Radom, L. *J. Am. Chem. Soc.* **2006**, *128*, 16004. (b) Wetmore, S. D.; Smith, D. M.; Bennett, J. T.; Radom, L. *J. Am. Chem. Soc.* **2002**, *124*, 14054.
- (15) (a) Smith, D. M.; Golding, B. T.; Radom, L. *J. Am. Chem. Soc.* **1999**, *121*, 1037. (b) Smith, D. M.; Golding, B. T.; Radom, L. *J. Am. Chem. Soc.* **1999**, *121*, 9388.
- (16) Frisch, M. J.; et al. *Gaussian 03*, revision C.02; Gaussian, Inc.: Wallingford, CT, 2004.